Research Article

How to cite this article: Esimbekova AR, Belenyuk VD, Savchenko AA, Ruksha TG. Vemurafenib Induces Senescent Phenotype with Increased Adhesion in BRAF Mutant A375 but not in Wild Type BRAF SK-MEL-2 Melanoma Cells. Advanced Pharmaceutical Bulletin, doi: 10.34172/apb.42808

Research Article
doi: 10.34172/apb.42808

Vemurafenib Induces Senescent Phenotype with Increased Adhesion in BRAF Mutant A375 but not in Wild Type BRAF SK-MEL-2 Melanoma Cells

Aleksandra Rashidovna Esimbekova[1], Vasiliy Dmitrievich Belenyuk[2], Andrey Anatolievich Savchenko[2], Tatiana Gennadievna Ruksha[1]*

[1]Department of Pathophysiology, Krasnoyarsk State Medical University, Krasnoyarsk, 660022, Russia.
[2]Laboratory of Cell Molecular Physiology and Pathology, Federal Research Center, Krasnoyarsk Science Center of the Siberian Branch of the Russian Academy of Sciences, Krasnoyarsk, 660022, Russia.

Running title: Vemurafenib induces senescence

***Correspondence: Tatiana Ruksha, Email: tatyana_ruksha@mail.ru**

Esimbekova : https://orcid.org/0000-0001-6363-5941
Savchenko : https://orcid.org/0000-0001-5829-672X
Ruksha : https://orcid.org/0000-0001-8142-4283

Submitted: June 22, 2024
Revised: January 06, 2025
Accepted: February 03, 2025
ePublished: February 12, 2025

Introduction

Cutaneous melanoma is a result of the neoplastic transformation of melanocytes and is the most lethal cancer among cutaneous malignancies. About 50% of cutaneous melanomas contain activated V600 mutations in the *BRAF* gene encoding serine-threonine protein kinase BRAF.[1] In 2011, the Food and Drug Administration (FDA) approved PLX4032, also known as vemurafenib, for the treatment of melanoma.[2] Small molecule BRAF inhibitor vemurafenib (PLX4032) has revolutionised melanoma therapy by inducing rapid tumour regression. However, > 50% of patients treated with vemurafenib monotherapy experience tumour recurrence within 6-7 months after the treatment.[3,4]

Emerging drug resistance poses a significant problem to effective treatment in oncology. The ability of tumour cells to enter the G_0 phase of the cell cycle, rendering them resistant to therapy, considered as one of the drug resistance mechanisms.[5] Most antitumour drugs target rapidly proliferating cells and are ineffective against G_0-positive cells corresponding to quiescent/senescent cells.[6,7,8] The G_0 phase may harbour both reversibly quiescent and senescent cells. Quiescent cells are characterised by diminished metabolic activity and limited antigenic repertoire, whereas senescent cells exhibit specific pro-inflammatory senescence associated secretory phenotype. Cellular senescence is characterised by the specific activity of senescence-associated β-galactosidase (SA-β-gal). Senescent cells via release of senescence associated mediators remodel the tumour microenvironment, promoting a pro-inflammatory microenvironment.[9]

A previous study showed that targeted therapy alters the secretome of tumour cells exposed to drug stress, thereby developing resistance.[10] Such resistant cancer cells can reside in distant organs and later may promote metastasis formation. This latent state is known as 'tumour dormancy' and can last for decades. Non-proliferating or slow-cycling cancer cells interact with their microenvironment. Indubitably, microenvironment is a key modulator of tumour progression; thus, it is essential to assess the role of extracellular matrix (ECM) components in the development of drug resistance and tumour progression. The ECM represents the boundary between the tumour metastatic niche and normal tissue and can exert both tumorigenic and antitumour effects. Fibronectin is one of the key components of the ECM implicated in metastatic niche formation.[11] Accumulating evidence shows that cancer cell adhesion to ECM proteins, including fibronectin, contributes to drug resistance. Cell adhesion-

mediated drug resistance has been described in various tumours including multiple myeloma,[12,13] lung cancer[14] and uveal melanoma.[15] As tumour progression is influenced by microenvironment, communication between cancer cells and microenvironment provided by adhesion molecules influences cell proliferation, migration, invasion, drug resistance.
In this study, we evaluated how vemurafenib affects melanoma cells percentage in different phases of a cell cycle and its ability to induce senescence in melanoma cells.

Materials and Methods

Cell lines and culture conditions

Human cutaneous melanoma cell lines BRAF wild-type SK-MEL-2 (ATCC® HTB-68™, Manassas, USA) and BRAF V660E-mutated A375 (ATCC® CRL-1619™, Manassas, USA) were cultured in DMEM (PanEko, Moscow, Russia) with 10% foetal bovine serum (FBS) (HyClone; Cytiva, Logan, USA) and 1% antibiotic/antimycotic (Gibco; Thermo Fisher Scientific, Inc., Carlsbad, USA), in an incubator at 37 °C under 5% CO_2 (Sanyo MSO-5AC, Tokyo, Japan). The cells were passaged at 80% confluency.

$BRAF^{V600E}$ mutation analysis

The mutational status of A375 and SK-MEL-2 melanoma cells was verified using the quantitative real-time PCR (qRT-PCR) BRAF-V600E kit (Biolink, Novosibirsk, Russia). DNA was extracted from cell cultures using the DNA extraction diaGene kit (Diam, Moscow, Russia) and estimated on a Qubit 2.0 fluorimeter (Invitrogen by Life Technologies, Singapore, Singapore) using an ssDNA HS Qubit analysis kit (Invitrogen, Eugene, OR, USA). The $BRAF^{V600E}$ mutation was evaluated by allele-specific real time PCR, as described previously.[16]

Cell viability assay

The half-maximal inhibition (IC_{50}) and maximum inhibition ($2IC_{50}$) concentrations of vemurafenib (Selleck Chemicals LLC, Houston, USA) were evaluated in melanoma cell lines A375 and SK-MEL-2 using the MTT (3-[4,5-dimethylthiazol-2-yl]-2,5 diphenyl tetrazolium bromide) method. The MTT is converted into water-insoluble formazan by mitochondrial dehydrogenases of viable cells. Cells were plated in 96-well microtiter plates at a density of 2×10^4 cells/mL and cultured overnight for cell attachment. Then, the medium was replaced with that containing 0–10 µM vemurafenib, and the culturing was continued at 37 °C under 5% CO_2 for 72 h. Subsequently, 5 mg/mL MTT reagent (Invitrogen, the Netherlands) was added to each well for 4 h. Finally, the reaction was quenched with 100 µL dimethyl sulfoxide (DMSO; Helicon, Moscow, Russia). The optical density was measured at 560 nm on an Efos-9305 spectrophotometer (Shvabe Photosystems, Moscow, Russia). The IC_{50} value was corresponded to 50 percent drop of metabolic activity. The assay was carried out in three biological replicates.

Vemurafenib treatment

Vemurafenib (PLX4032) was obtained from Selleck Chemicals LLC. Melanoma cells were treated with 0.45 µM and 0.9 µM for the A375 cell line, 1.7 µM and 3.4 µM for the SK-MEL-2 line corresponding to IC_{50} and $2IC_{50}$ of vemurafenib, respectively, for 3 days, washed with phosphate-buffered saline (PBS; Helicon, Moscow, Russia) and cultured for 48 h. On day 5 after the treatment, the cells were harvested for further experiments. DMSO served as the negative control, the cells were treated with DMSO in an independent well concurrent to vemurafenib.

Cell cycle analysis

The distribution of cells across cell cycle phases was assessed by propidium iodide (PI) staining and monoclonal antibodies against Ki-67. Cells were treated with vemurafenib at IC_{50} and $2IC_{50}$ concentrations, washed with PBS (Helicon), fixed with 70% ice-cold ethanol, permeabilized with 0.1% Triton X100 (Biotechnik GmbH, Geiberg, Germany) and treated with RNase A (100 µg/mL) (Invitrogen, Thermo Fisher Scientific, Vilnius, Lithuania). Then, the cells were stained with anti-Ki-67 monoclonal antibodies labelled by FITC (clone: SolA15, eBioscience, Thermo Fisher Scientific, Carlsbad, USA) at a concentration of 1:100 and 100 µg/mL PI (Invitrogen, Thermo Fisher Scientific, Carlsbad, USA), followed by incubation at 37 °C in the dark for 1 h. The percentage of cells in each phase of the cell cycle was determined on a Cytomics FC-500 flow cytometer (Beckman Coulter, Fullerton, USA) and CXP software (version 2.2; Beckman Coulter, Brea, USA) based on the differences in Ki-67 expression level and RNA content of the cells, which was characterised by PI staining. Typically, cells in the G_0 phase were characterised by diminished Ki-67 levels and RNA content, which distinguishes them from proliferating cells. Gating was carried out in the fluorescence range Ki-67-FITC ≤ 100 (negative) and in the fluorescence range PI from 0.7 to 1.3 relative units. The experiment was done in three biological replicates.

Immunocytochemistry

The immunocytochemical study was performed using the cell proliferation marker Ki-67 to determine the portion of cells residing in the G_0 phase of the cell cycle. Cells were incubated with vemurafenib at IC_{50} and $2IC_{50}$ concentrations, fixed with 10% formaldehyde and permeabilized with 0.5% Triton X-100 (Biotechnik GmbH, Geiberg, Germany). Then primary rabbit monoclonal antibodies to human Ki-67 (1:100; ab15580; Abcam, Cambridge, USA) in 10% FBS (HyClone, GmbH, Parsching, Austria) were applied at 4 °C overnight. Secondary

goat anti-rabbit antibody labelled with Alexa Fluor 488 (Invitrogen, Thermo Fisher Scientific, Eugene) were used at a dilution 1:200 for 1 h. DAPI (AppliChem GmbH, Darmstadt, Germany) at concentration 1 μg/mL was used for 15 min. The proportion of Ki-67-positive cells was evaluated in at least ten fields on a Floid Cell Imaging Station (Thermo Fisher Scientific, Bothell, USA). Proliferating cells were considered as cells with nuclei stained green and blue, whereas non-proliferating G_0-positive cells were characterised by blue nuclei.

Detection of β-galactosidase activity

In order to determine the level of vemurafenib-induced senescent melanoma cells, the activation of β-galactosidase was evaluated. This cytochemical analysis was based on staining the cells containing the active enzyme with the chromogen X-gal (5-bromo-4-chloro-3-indoyl β-d-galactopyranoside). The cells were cultured with vemurafenib at IC_{50} and $2IC_{50}$ concentrations, fixed with 4% formaldehyde and stained in the dark at 37 °C. The staining buffer included 1X citric acid/sodium phosphate buffer (pH 6.0) (Abcam, UK), 5 mmol potassium hexacyanoferrate (III) (AO Reakhim, Moscow, Russia), 5 mmol potassium hexacyanoferrate (II) (AO Reakhim), 150 mmol NaCl (JSC Reakhim), 2 mmol MgCl2 (JSC Reakhim) and 1 mg/mL 5-bromo-4-chloro-3-indolyl β-D-galactopyranoside (Invitrogen; Thermo Fisher Scientific). X-gal undergoes hydrolysis in the presence of active β-galactosidase to form a blue product visualised under a microscope (MIB-R; LOMO-Microsystems, Saint Petersburg, Russia).

Centrifugal cell adhesion assay

Vemurafenib-treated melanoma cells were cultured at a density of 2×10^5 cells/mL in the culture flasks. Then they were filled with PBS and subjected to centrifugation upward in a monolayer at 1000 rpm for 3 min. Then the cells were washed with PBS, fixed with 10% formaldehyde and permeabilized with 0.5% Triton X-100 (Biotechnik GmbH, Geiberg, Germany). Then cells were subjected to incubation with anti-Ki-67 monoclonal antibodies (1:100; ab15580; Abcam) overnight at 4 °C followed by the application of a secondary IgG goat antibody conjugated with Alexa Fluor 488 (H + L) (1:100; Invitrogen, Thermo Fisher Scientific, Eugene, USA) at room temperature in the dark for 90 min. Cells were incubated with DAPI (1:10,000) for 15 min. The percentage of Ki-67-negative cells was assessed on a Floyd Cell Imaging Station. Ki-67-negative cells were characterised by blue nuclei.

Adhesion to fibronectin

A fibronectin human plasma solution (100 μg/mL) (Sigma-Aldrich, St. Louis, USA) was dispensed into a 96-well plate to create an adhesive substrate, while wells without coating served as controls. The wells were rinsed with sterile PBS before seeding the cells at a density of 3×10^4 cells/mL for 2.5 h in a CO_2 incubator; the nonadherent cells were discarded, and the cells were washed with PBS before staining with methylene blue. The optical density of adherent fibronectin cells was measured at 620 nm on an Efos-9305 spectrophotometer (Shvabe Photosystems, Moscow, Russia).

qPCR real time

Total RNA was isolated from cells using the RNA isolation kit (Diam, Moscow, Russia). The RNA concentration was measured on a Qubit 2.0 fluorimeter (Invitrogen by Life Technologies, Singapore) using the HS Qubit RNA analysis kit (Invitrogen, Eugene, Oregon, USA). Moloney murine leukaemia virus (MMLV) RT kit (Eurogen, Moscow, Russia) was used for cDNA synthesis by reverse transcription reaction. The qRT-PCR reaction mixture consisted of a 2.5X Master Mix with ROX (Syntol, Moscow, Russia), deionised water and 20X primer TaqMan™ Gene Expression Assay: CCND1 Hs00765553_m1, RBL1 Hs00765700_m1 (cat. no. 4331182, Applied Biosystems, Pleasanton, USA). The primers for adhesion molecules expression evaluation were as follows: *ITGA5* (Ensembl: ENSG00000161638), *ITGAV* (Ensembl: ENSG00000138448), *ITGB1* (Ensembl: ENSG00000150093) and *ITGB3* (Ensembl: ENSG00000259207). The amplification was carried out on a Step One™ real-time PCR device (Applied Biosystems, Singapore, Singapore). Amplification regime included 50 °C for 2 min, 95 °C for 10 min and 40 cycles at 95 °C for 15 s and 0 °C for 1 min. *GAPDH* (Ensembl: ENSG00000111640) and *HPRT* (Ensembl: ENSG00000165704) were used as endogenous controls. All the aforementioned primers were synthesised by DNA Synthesis Ltd (Moscow, Russia). The data were analysed with the use ΔΔCt method. The assay was carried out in three technical replicates.

Statistical analysis

Statistical analyses were conducted using Statistica 7.0 (StatSoft, Inc., Statistics, USA). GraphPad Prism (v8; GraphPad Software, Inc.; https://www.graphpad.com/) was used to generate the graphs. $p < 0.05$ was considered as statistically significant. All the experimental procedures were conducted in three biological replicates.

Results

Allele-specific real-time PCR determined that the Ct value for DNA isolated from SK-MEL-2 cells was 39.77, whereas that of the DNA isolated from A375 cells was 19.15, similar to the positive control DNA. Therefore, we

speculated that A375 melanoma cells harbour *BRAF* V600E mutation, whereas SK-MEL-2 cells characterised by wild-type *BRAF* (Figure 1).

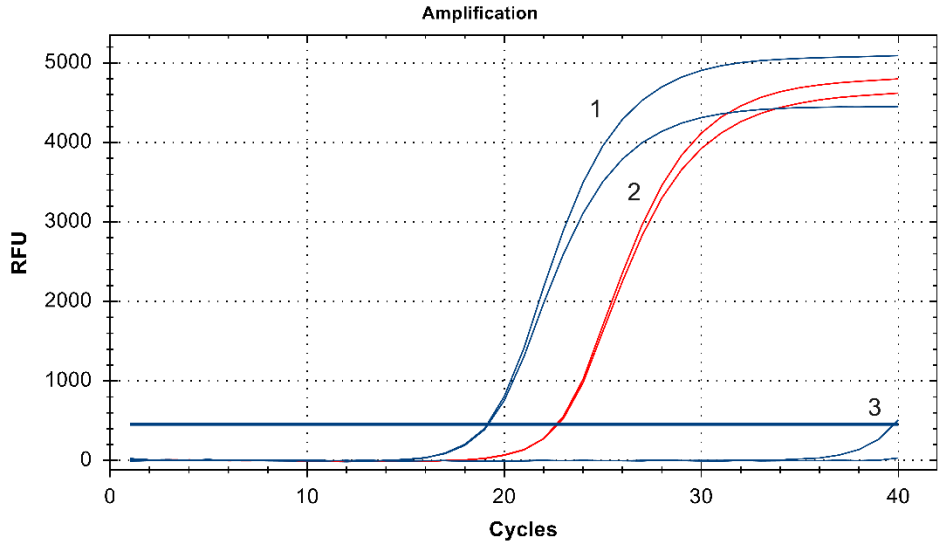

Figure 1. Mutational status of A375 and SK-MEL-2 melanoma cells determined by allele-specific real-time PCR. The Ct value of DNA isolated from A375 cells was 19.15 (1), which was similar to the Ct value of the positive control (2), whereas the Ct value of DNA isolated from SK-MEL-2 cells was 39.77 (3).

The MTT assay showed that $BRAF^{mt}$ A375 and $BRAF^{wt}$ SK-MEL-2 vemurafenib treatment decreased the metabolic activity with increasing vemurafenib concentration. IC_{50} and $2IC_{50}$ of vemurafenib were 0.45 µM and 0.9 µM for the A375 melanoma cells and 1.7 µM and 3.4 µM for the SK-MEL-2 cells, respectively (Figure 2).

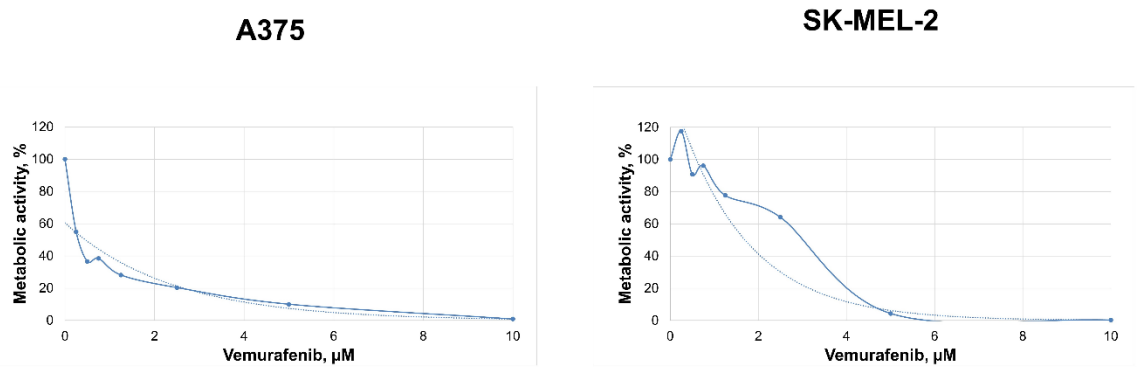

Figure 2. Changes in the metabolic activity of cutaneous melanoma cells $BRAF^{mt}$ A375 and $BRAF^{wt}$ SK-MEL-2 depending on the concentration of vemurafenib demonstrated by the MTT assay.

Then, vemurafenib at concentrations IC_{50} and $2IC_{50}$, was added to A375 and SK-MEL-2 to determine the effects of the drug on cell cycle phase distribution by flow cytometry using PI and anti-Ki-67-FITC monoclonal antibodies.

The level of apoptotic $BRAF^{mt}$ A375 cells corresponding to cells residing in pre-G_0 phase increased by 2.3 times after treatment with 0.45 µM vemurafenib (IC_{50}) and by 2.4 times after 0.9 µM vemurafenib ($2IC_{50}$). Conversely, $1IC_{50}$ and $2IC_{50}$ concentrations of vemurafenib induced a 1.7- and 1.5-fold decrease, respectively, in apoptotic cells in $BRAF^{wt}$ SK-MEL-2 cell line. The flow cytometry analysis of PI-stained cells showed an increased proportion of $BRAF^{mt}$ A375 cells residing in G_0-G_1 phases from 77.42% to 89.81% and 90.28% in response to vemurafenib treatment at 0.45 µM and 0.9 µM, respectively, whereas the cell percentage was decreased in the G_2-M and S phases. On the other hand, vemurafenib decreased the percentage of cells in the S phase and slightly increased the proportion of $BRAF^{wt}$ SK-MEL-2 cells in the G_2-M phase (Figure 3A).

Ki-67 staining with subsequent flow cytometry revealed that vemurafenib increased the proportion of $BRAF^{mt}$ A375 cells from 79.15% to 92.92% (IC_{50}) and 93.27% ($2IC_{50}$) in the G_1 phase, followed by 2.9 times by $1IC_{50}$ and 3.4 times by $2IC_{50}$ decrease in the G_2 phase of the cell cycle (Figure 3B).

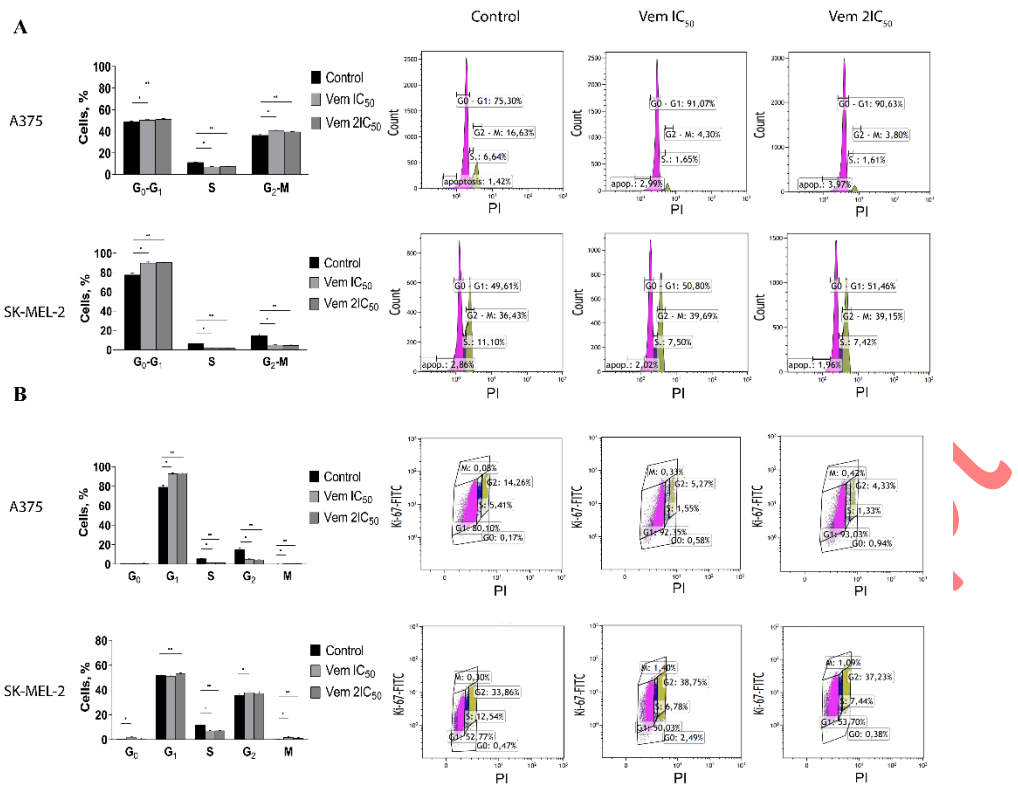

Figure 3. Changes in cell ratio corresponding to the cell cycle phase under the influence of vemurafenib IC_{50} and $2IC_{50}$ concentrations on $BRAF^{mt}$ A375 and $BRAF^{wt}$ SK-MEL-2 cutaneous melanoma cells shown by the results of flow cytometry with PI (A). Changes in the ratio of cells corresponding to the phase of the cell cycle under the vemurafenib IC_{50} and $2IC_{50}$ concentrations on cutaneous melanoma cells of the $BRAF^{mt}$ A375 and $BRAF^{wt}$ SK-MEL-2 cell lines according to the results of flow cytometry with Ki-67-FITC and PI (B).

The visualisation of Ki-67 staining revealed a significant increase in the percentage of Ki-67-negative $BRAF^{mt}$ A375 cells that corresponded to G_0-positive cells: from 4.31% to 31.82% after treatment with 0.45 μM vemurafenib (IC_{50}) and 62.46% after treatment with 0.9 μM vemurafenib ($2IC_50$). However, flow cytometry showed an elevation in the cells corresponded to the G_1 phase. Interestingly, the variable expression of Ki-67 in the G_1 makes it challenging to differentiate the G_1 and G_0 phases.[17] Immunocytochemistry showed an increase in the percentage of G_0-positive $BRAF^{mt}$ A375 cells, while that of G_0-positive $BRAF^{wt}$ SK-MEL-2 cells remained unchanged (Figure 4A).

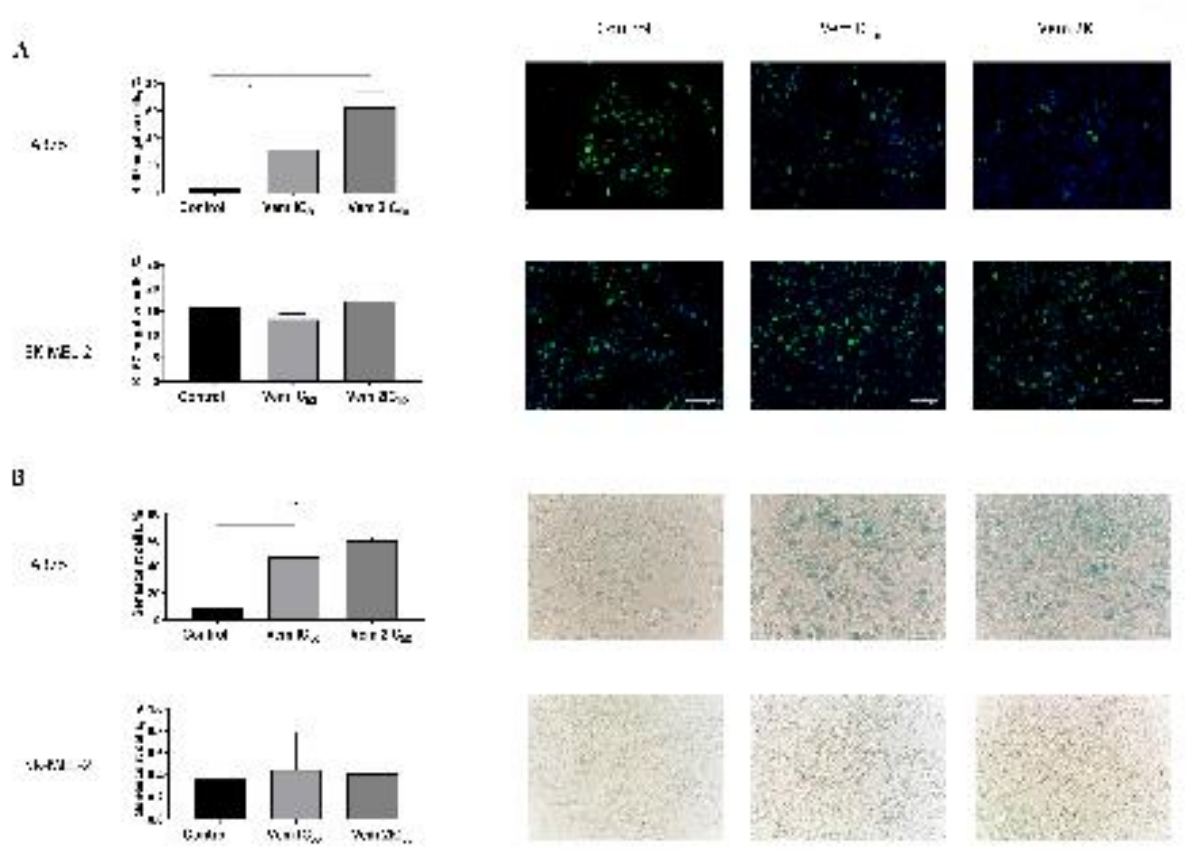

Figure 4. Immunocytochemistry of cutaneous melanoma cell lines $BRAF^{mt}$ A375 and $BRAF^{wt}$. SK-MEL-2 stained with Ki-67 antibodies and DAPI after exposure to vemurafenib concentrations IC_{50} and $2IC_{50}$, wherein the nuclei of Ki-67-positive cells are green, and the nuclei of Ki-67-negative, G_0-positive cells are blue (A).
Altered proportion of $BRAF^{mt}$ A375 and $BRAF^{wt}$ SK-MEL-2 cutaneous melanoma cells expressing β-galactosidase following exposure to vemurafenib IC_{50} and $2IC_{50}$ concentrations, wherein β-galactosidase-positive cells, termed senescent cells, are visualised as blue coloured (B).
Note: * $p < 0.05$ – statistically significant differences between cells exposed to vemurafenib IC_{50} concentration and control.
** $p < 0.05$ – statistically significant differences between cells exposed to vemurafenib concentration $2IC_{50}$ and control.

The G_0 phase of the cell cycle consists of both quiescent cells that retain the ability of proliferation and senescent cells that characterized by permanent exit from a cell cycle followed by elimination through apoptosis. Then, the cells were subjected to 5-bromo-4-chloro-3-indolyl β-D-galactopyranoside, a substrate for β-galactosidase. The positive cells were stained blue (Figure 4B). Under 0.45 μM (IC_{50}) vemurafenib treatment, the rate of senescent (β-galactosidase-positive) $BRAF^{mt}$ A375 cells was increased from 9.75% to 47.24%, whereas 0.9 μM ($2IC_{50}$) vemurafenib increased the cell content up to 59.86%; however, the level of β-galactosidase-positive $BRAF^{wt}$ SK-MEL-2 cells under vemurafenib treatment remained unchanged. In order to confirm the transition of the melanoma cells to a senescent state under vemurafenib treatment, we analysed the expression and evaluated the mRNA levels of cyclin D1 (*CCND1*) and *RBL1*. The results showed decreased levels of *CCND1* and *RBL1* in A375 cells. Instead, SK-MEL-2 cells were characterised by upregulated levels of both molecules (Figure 5).

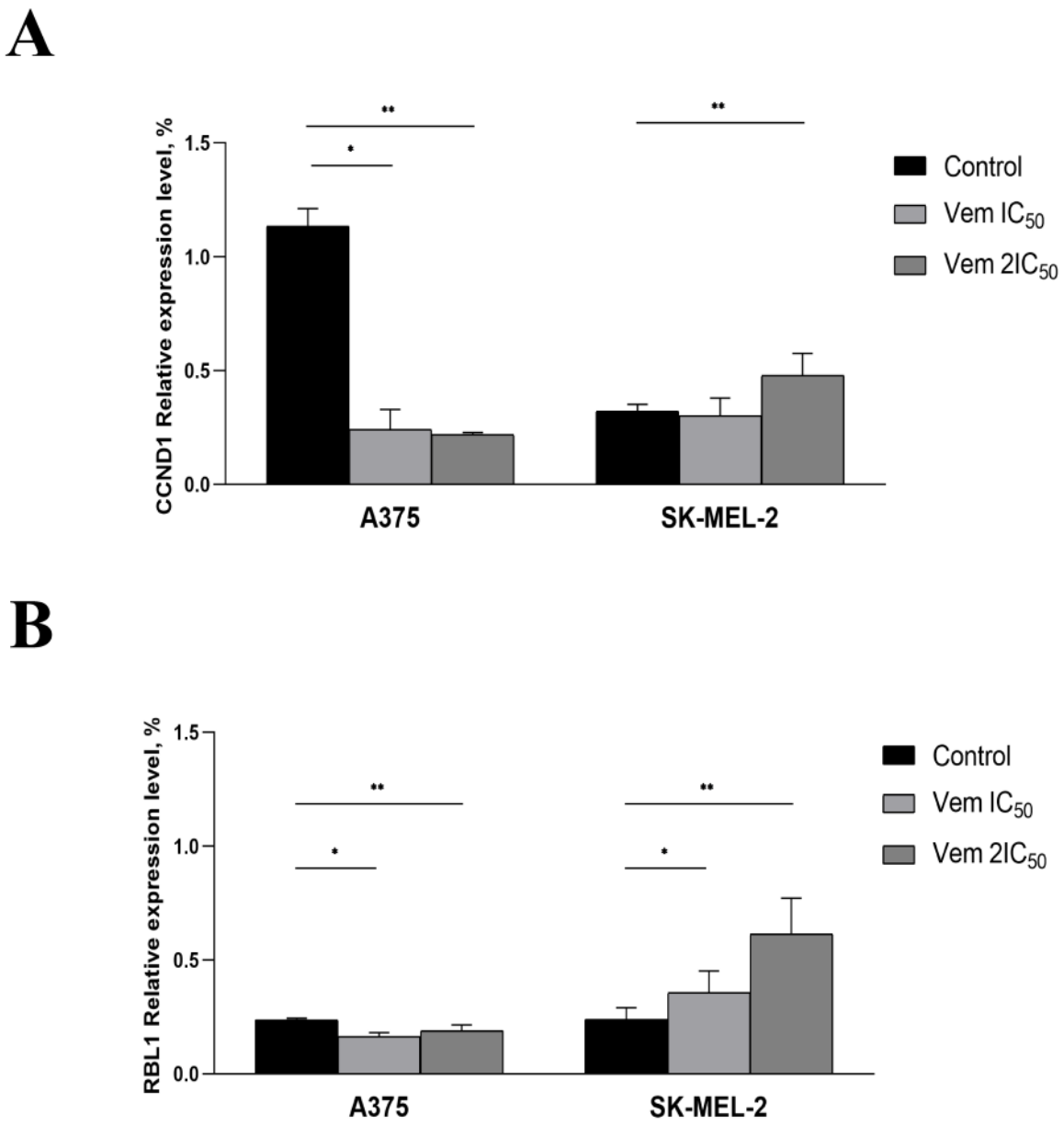

Figure 5. Relative *CCND1* (A) and *RBL1* (B) gene expression levels under vemurafenib treatment at 0.45 µM ($1IC_{50}$) and 0.9 µM ($2IC_{50}$) for A375 cell line, 1.7 µM (IC_{50}) and 3.4 µM ($2IC_{50}$) for the SK-MEL-2 melanoma cells.
Note: * $p < 0.05$ – statistically significant differences between cells exposed to vemurafenib at $1xIC_{50}$ concentration and control.
** $p < 0.05$ – statistically significant differences between cells exposed to vemurafenib $2IC_{50}$ concentration and control.

Furthermore, an increase in the percentage of G_0-positive senescent $BRAF^{mt}$ A375 cells was correlated with increased cell adhesion abilities, as determined by enhanced adhesion to the surface of the culture flask under centrifugation (Figure 6A). 0.45 µM vemurafenib ($1IC_{50}$) and 0.9 µM vemurafenib (2) treatment of $BRAF^{mt}$ A375 cells increased the percentage of adherent cells from 55.27% to 66.6% and 79.05% after centrifugation. Also, an increased proportion of G_0-positive cells was observed in melanoma cells attached to the bottom of the flask post-centrifugation. The percentage of attached Ki-67-negative cells was 0.13% cells in the control and was 32.74% in 0.45 µM vemurafenib-treated cells and 60.19% in 0.9 µM vemurafenib-treated cells (Figure 6B). BRAF-negative SK-MEL-2 cells exhibited neither an increase in senescent cell proportion under vemurafenib treatment nor an increase in Ki-67-negative cells. The value of the optical density of BRAF-positive A375 melanoma cells attached to fibronectin was increased 1.87 times, whereas BRAF-negative SK-MEL-2 cells did not show any alteration in adhesion to fibronectin after vemurafenib treatment (Figure 6C).

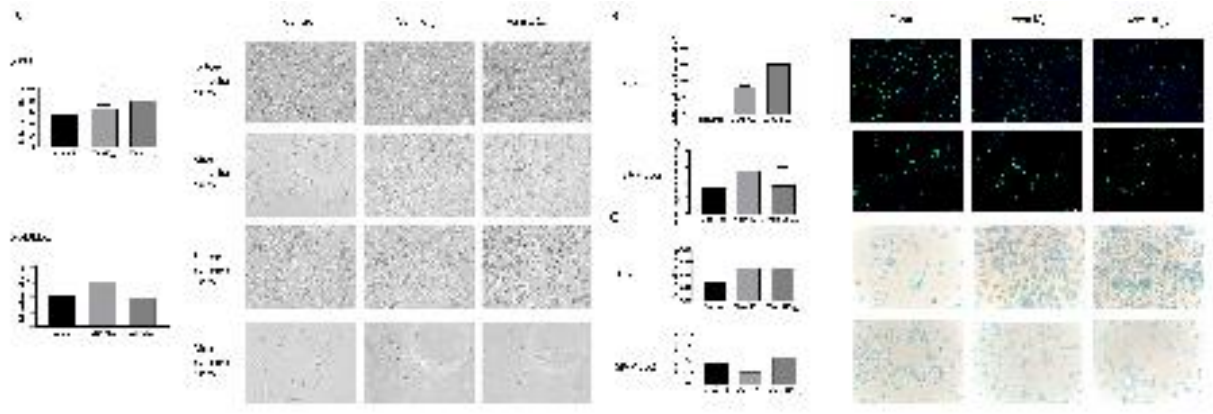

Figure 6. Adhesive capacities of cutaneous melanoma $BRAF^{mt}$ A375 and $BRAF^{wt}$ SK-MEL-2 cells after exposure to vemurafenib at concentrations corresponding to IC_{50} and $2IC_{50}$ determined by centrifugal force application (A). Immunocytochemical study of adherent cutaneous melanoma cells line $BRAF^{mt}$ A375 and $BRAF^{wt}$ SK-MEL-2 after treatment with vemurafenib corresponding to the $1IC_{50}$ and $2IC_{50}$ concentrations after centrifugal force application (B). Adhesion of $BRAF^{mt}$ A375 and $BRAF^{wt}$ SK-MEL-2 cutaneous melanoma cells to fibronectin after treatment with vemurafenib corresponding to $1IC_{50}$ and $2IC_{50}$ concentrations (C).
Note: * $p < 0.05$ – statistically significant differences between cells exposed to dacarbazine at $1IC_{50}$ concentration and control.
** $p < 0.05$ – statistically significant differences between cells exposed to vemurafenib concentration $2IC_{50}$ and control.

Cancer cells interact with fibronectin via integrins: ITGAV, ITGA5, ITGB1 and ITGB3. Therefore, the levels of these integrins were evaluated in A375 and SK-MEL-2 after vemurafenib exposure. Consequently, 2xIC vemurafenib upregulated ITGAV and ITGB3 mRNA levels in both A375 and SK-MEL-2 cells but downregulated ITGB1 and ITGB3 expression levels in A375. ITGA5 was increased in A375 but decreased in SK-MEL-2 cells post vemurafenib treatment at IC_{50} and $2IC_{50}$ concentrations (Figure 7).

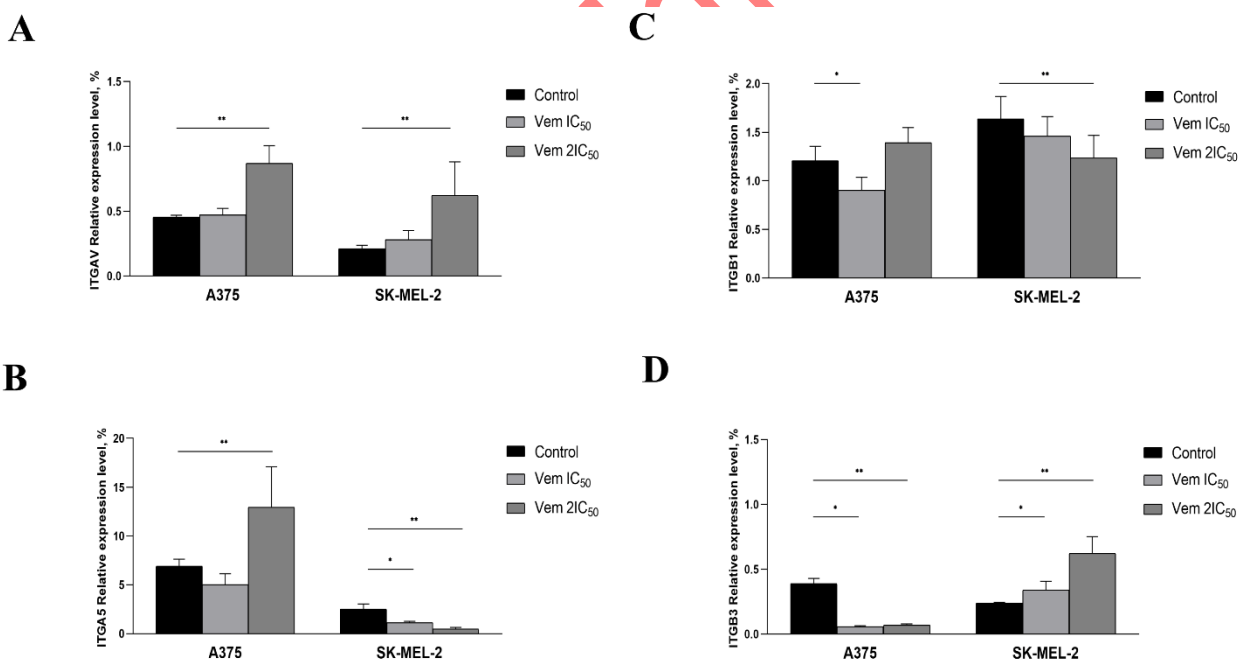

Figure 7. Altered expression levels of *ITGAV* (A), *ITGA5* (B), *ITGB1* (C) and *ITGB3* (D) under vemurafenib treatment at 0.45 µM (IC_{50}) and 0.9 µM ($2IC_{50}$) for A375, 1.7 µM (IC_{50}) and 3.4 µM ($2IC_{50}$) for SK-MEL-2.
Note: * $p < 0.05$ – statistically significant differences between cells exposed to vemurafenib concentration corresponding to IC_{50} concentration and control.
** $p < 0.05$ – statistically significant differences between cells exposed to vemurafenib concentration corresponding to $2IC_{50}$ and control.

Thus, BRAF-positive melanoma cells that remained viable after exposure to vemurafenib exhibited characteristics of senescent tumour cells and increased adhesive properties due to fibronectin binding. Wild-type *BRAF* gene harbouring melanoma cells exhibited neither the characteristics of senescent cells nor changes in adhesion levels.

Discussion

Melanoma resistance to molecular targeted therapy was observed after implementing BRAF inhibitors into clinical practice. However, several mechanisms have been associated with melanoma drug resistance to vemurafenib. Thus, vemurafenib-resistant cells characterised by mitogen-activated protein kinase (MAPK)

reactivation through expression of aberrantly spliced mutated BRAF protein exhibiting kinase activity.[18] Also, other mechanisms of melanoma BRAF resistance underlie BRAF amplification.[19] and the activation of the prooncogenic signalling pathway.[20]

Melanoma is recognised as a highly plastic tumour system, wherein multiple processes are activated in response to anticancer drug application. Cancer cell plasticity is a mechanism for phenotype modification to adapt and survive in an unfavourable environment for further progression and metastasis. A recent study showed that cancer cells escape immune evasion and apoptosis-inducing stimuli by transient transition from the cell cycle to the quiescent state corresponding to the G_0 phase of the cell cycle.[21] Thus, understanding cell cycle associated resistance mechanisms is essential to developing effective personalised, targeted therapies.

Vemurafenib blocks the activation of MAPKs with V600E mutation through ATP-competitive inhibition of the kinase domain of BRAF. Although vemurafenib is more specific than cytotoxic chemotherapeutic agents, it may also exert off-target effects.[22] In the current study, vemurafenib inhibits the proliferative activity of $BRAF^{WT}$ SK-MEL-2 cells but at a concentration four times higher than in $BRAF^{V600E}$ A375 cells.

Our results showed that vemurafenib induces exit from the cell cycle concurrent to shifting BRAF-positive melanoma cells from proliferative to senescent state that was evaluated by histochemical assay detecting the β-galactosidase activity and the altered expression levels of cell cycle-related proteins — CCND1 and RBL1. CCND1 interacts with cyclin-dependent kinase 4 or 6, followed by retinoblastoma protein inactivation essential for cell cycle transition from the G_1 to the S phase.[23] As observed previously, we also showed that CCND1 depletion is associated with cancer cell transition to a senescent state.[24] The hyperphosphorylated form of RBL1 interacts with the transcription factors to repress the transcription of genes implicated in cell cycle progression.[25] Moreover, RBL1 downregulation is linked to the transition to the senescent state.[26] Therefore, both cell cycle-related genes — *CCND1* and *RBL1* — exhibited altered expression patterns accompanying a shift to the senescent state.

Senescence is defined as permanent cell cycle arrest followed by apoptosis development. However, recent studies found that the senescent state is a reversible condition. It is in the line with our study indicated that melanoma cells resistant to the proapoptotic effect of vemurafenib are characterised by reduced proliferation and increased β-galactosidase activity, which are characteristics of senescent cells. Senescence facilitates stress-responsive cancer cells to adapt to altering environmental conditions primarily via epigenetic reprogramming.[27] Our previous studies revealed that dacarbazine-induced melanoma cells exit from the cell cycle accompanied by transcriptional activation of focal adhesion signalling and enhanced adhesive capacities.[24] Additionally, resting BRAF-positive melanoma cells treated with BRAF inhibitor exhibited similar phenotypic features. In the present study, we observed that G_0-positive but senescent melanoma cells adhere to surfaces post-centrifugation. Moreover, these cells exhibit facilitated interaction with fibronectin. Strikingly, the adhesive capacities and interaction with fibronectin remained unchanged in vemurafenib-treated BRAF-negative melanoma cells.

ECM is a critical regulator of disseminated cancer cells' reprogramming during their migration, intra- and extravasation and further seeding in distant organs. However, whether ECM supports quiescent cell reactivation is yet to be clarified. Fluegen et al. showed that hypoxic ECM favours the shift of proliferative cancer cells to a quiescent state.[28] Urokinase receptor interaction with □5□1 integrin stimulates cancer cell adhesion to fibronectin, stimulating ERK-mediated cell proliferation.[29] Thus, increased adhesive features in senescent melanoma cells represent phenotypic reprogramming and essential features to maintain the quiescent state or balance between proliferative and cell arrest stimuli.

Among ECM components, fibronectin is a key player that establishes the premetastatic niche.[11] It is involved in tumour progression, drug resistance and metastasis development in various solid tumours.[30,31,32,] Fibronectin interaction with circulated cancer cells via focal adhesion protein Talin1 facilitates the formation of a premetastatic niche in the liver[33] and promotes epithelial-mesenchymal transition, migration and invasion in MCF-7 breast cancer cells.[34] A recent study established that fibronectin-dependent compression of tumour cells by cancer-associated fibroblasts reduces the transcription factor YAP-mediated cancer cell proliferation.[35] ITGAV (also known as CD51) is shown to be a marker of colorectal cancer stem cells. In addition, ITGAV-positive cancer cells demonstrated chemoresistance to 5-fluorouracil (5-FU) and oxaliplatin.[36] This observation was in line with the current results showing increased ITGAV levels in viable BRAF-positive melanoma cells after vemurafenib treatment. On the other hand, ITGAV triggers the transforming growth factor-beta following epithelial-mesenchymal transition activation. This phenomenon corresponded to our previous results that non-apoptotic BRAF-positive primary melanoma cells were characterized by enhanced migratory and invasive capacities after vemurafenib treatment.[16] Recent data presumed that senescent cells have the potency to return to the proliferative state.[37] Moreover, non-dividing cancer cells express various phenotypes, resulting in a heterogeneous population of slow-cycling cells[16]

Taken together, the current observations provide an in-depth insight into vemurafenib-associated cancer cell resistance, thereby enhancing our understanding of tumour cell plasticity induced by anticancer agents.

Conclusion

Vemurafenib induces senescence in $BRAF^{V600E}$ melanoma cells, avoiding apoptosis. Senescent cells were characterised by increased adhesive capacities and binding to fibronectin that corresponds to ITGAV expression

increase. Our findings reflect the phenotypic drug-resistance and non-proliferating cancer cell interaction with the ECM matrix for survival. Thus, targeting senescent cells by focal adhesion modulators can be considered further as possible approach to optimize treatment modalities in melanoma patients..

Competing Interests
The authors declare no conflict of interest

Authors' Contribution
Conceptualization: Tatiana Ruksha.
Data curation: Tatiana Ruksha.
Formal analysis: Aleksandra Esimbekova, Vasiliy Belenyuk.
Funding acquisition: Tatiana Ruksha.
Investigation: Aleksandra Esimbekova.
Methodology: Tatiana Ruksha, Aleksandra Esimbekova, Vasiliy Belenyuk, Andrey Savchenko.
Project administration: Tatiana Ruksha.
Resources: Vasiliy Belenyuk, Andrey Savchenko.
Software: Aleksandra Esimbekova, Vasiliy Belenyuk.
Supervision: Tatiana Ruksha.
Validation: Aleksandra Esimbekova.
Visualization: Aleksandra Esimbekova.
Writing–original draft: Aleksandra Esimbekova, Tatiana Ruksha.
Writing–review & editing: Tatiana Ruksha.

Funding
This research was funded by Russian Science Foundation, grant number 19-15-00110, https://rscf.ru/project/19-15-00110/.

Acknowledgments
Graphic abstract was created with BioRender.com (https://biorender. com/).

Ethical issues

References
1. Aksenenko MB, Kirichenko AK, Ruksha TG. Russian study of morphological prognostic factors characterization in BRAF-mutant cutaneous melanoma. *Pathol Res Pract*. 2015;211(7):521-527. doi: 10.1016/j.prp.2015.03.005
2. Ascierto PA, Kirkwood JM, Grob JJ, Simeone E, Grimaldi AM, Maio M, Palmieri G, Testori A, Marincola FM, Mozzillo N. The role of BRAF V600 mutation in melanoma. *J Transl Med*. 2012;10:85. doi: 10.1186/1479-5876-10-85
3. Sosman JA, Kim KB, Schuchter L, Gonzalez R, Pavlick AC, Weber JS, McArthur GA, Hutson TE, Moschos SJ, Flaherty KT, Hersey P, Kefford R, Lawrence D, Puzanov I, Lewis KD, Amaravadi RK, Chmielowski B, Lawrence HJ, Shyr Y, Ye F, Li J, Nolop KB, Lee RJ, Joe AK, Ribas A. Survival in BRAF V600-mutant advanced melanoma treated with vemurafenib. *N Engl J Med*. 2012;366(8):707-714. doi: 10.1056/NEJMoa1112302
4. Chapman PB, Hauschild A, Robert C, Haanen JB, Ascierto P, Larkin J, Dummer R, Garbe C, Testori A, Maio M, Hogg D, Lorigan P, Lebbe C, Jouary T, Schadendorf D, Ribas A, O'Day SJ, Sosman JA, Kirkwood JM, Eggermont AM, Dreno B, Nolop K, Li J, Nel-son B, Hou J, Lee RJ, Flaherty KT, McArthur GA; BRIM-3 Study Group. Improved survival with vemurafenib in melanoma with BRAF V600E mutation. *N Engl J Med*. 2011;364(26):2507-2516. doi: 10.1056/NEJMoa1103782
5. Senft D, Ronai ZA. Immunogenic, cellular, and angiogenic drivers of tumor dormancy--a melanoma view. *Pigment Cell Melanoma Res*. 2016;29(1):27-42. doi: 10.1111/pcmr.12432
6. Mellor HR, Ferguson DJ, Callaghan R. A model of quiescent tumour microregions for evaluating multicellular resistance to chemotherapeutic drugs. *Br J Cancer*. 2005;93(3):302-309. doi: 10.1038/sj.bjc.6602710
7. Dias IB, Bouma HR, Henning RH. Unraveling the big sleep: molecular aspects of stem cell dormancy and hibernation. *Front Physiol*. 2021;12:624950. doi: 10.3389/fphys.2021.624950
8. Luk CK, Keng PC, Sutherland RM. Radiation response of proliferating and quiescent subpopulations isolated from multicel-lular spheroids. *Br J Cancer*. 1986;54(1):25-32. doi: 10.1038/bjc.1986.148
9. Ohtani N. The roles and mechanisms of senescence-associated secretory phenotype (SASP): can it be controlled by senolysis? *Inflamm Regen*. 2022;42(1):11. doi: 10.1186/s41232-022-00197-8

10. Obenauf AC, Zou Y, Ji AL, Vanharanta S, Shu W, Shi H, Kong X, Bosenberg MC, Wiesner T, Rosen N, Lo RS, Massagué J. Therapy-induced tumour secretomes promote resistance and tumour progression. *Nature*. 2015;520(7547):368-372. doi: 10.1038/nature14336
11. Chin AR, Wang SE. Cancer tills the premetastatic field: mechanistic basis and clinical implications. *Clin Cancer Res*. 2016;22(15):3725-3733. doi: 10.1158/1078-0432.CCR-16-0028
12. Hazlehurst LA, Argilagos RF, Emmons M, Boulware D, Beam CA, Sullivan DM, Dalton WS. Cell adhesion to fibronectin (CAM-DR) influences acquired mitoxantrone resistance in U937 cells. *Cancer Res*. 2006;66(4):2338-2345. doi: 10.1158/0008-5472
13. Shain KH, Dalton WS. Environmental-mediated drug resistance: a target for multiple myeloma therapy. *Expert Rev Hematol*. 2009 c;2(6):649-662. doi: 10.1586/ehm.09.55
14. Sethi T, Rintoul RC, Moore SM, MacKinnon AC, Salter D, Choo C, Chilvers ER, Dransfield I, Donnelly SC, Strieter R, Haslett C. Extracellular matrix proteins protect small cell lung cancer cells against apoptosis: a mechanism for small cell lung cancer growth and drug resistance in vivo. *Nat Med*. 1999;5(6):662-668. doi: 10.1038/9511
15. Bérubé M, Talbot M, Collin C, Paquet-Bouchard C, Germain L, Guérin SL, Petitclerc E. Role of the extracellular matrix proteins in the resistance of SP6.5 uveal melanoma cells toward cisplatin. *Int J Oncol*. 2005;26(2):405-413. doi: 10.3892/ijo.26.2.405
16. Komina AV, Palkina NV, Aksenenko MB, Lavrentev SN, Moshev AV, Savchenko AA, Averchuk AS, Rybnikov YA, Ruksha TG. Semaphorin-5A downregulation is associated with enhanced migration and invasion of BRAF-positive melanoma cells under vemurafenib treatment in melanomas with heterogeneous BRAF status. *Melanoma Res*. 2019;29(5):544-548. doi: 10.1097/CMR.0000000000000621.
17. Miller I, Min M, Yang C, Tian C, Gookin S, Carter D, Spencer SL. Ki67 is a graded rather than a binary marker of proliferation versus quiescence. *Cell Rep*. 2018;24(5):1105-1112.e5. doi: 10.1016/j.celrep.2018.06.110
18. Zhang C, Spevak W, Zhang Y, Burton EA, Ma Y, Habets G, Zhang J, Lin J, Ewing T, Matusow B, Tsang G, Marimuthu A, Cho H, Wu G, Wang W, Fong D, Nguyen H, Shi S, Womack P, Nespi M, Shellooe R, Carias H, Powell B, Light E, Sanftner L, Walters J, Tsai J, West BL, Visor G, Rezaei H, Lin PS, Nolop K, Ibrahim PN, Hirth P, Bollag G. RAF inhibitors that evade paradoxical MAPK pathway activation. *Nature*. 2015;526(7574):583-586. doi: 10.1038/nature14982
19. Johnson DB, Menzies AM, Zimmer L, Eroglu Z, Ye F, Zhao S, Rizos H, Sucker A, Scolyer RA, Gutzmer R, Gogas H, Kefford RF, Thompson JF, Becker JC, Berking C, Egberts F, Loquai C, Goldinger SM, Pupo GM, Hugo W, Kong X, Garraway LA, Sosman JA, Ribas A, Lo RS, Long GV, Schadendorf D. Acquired BRAF inhibitor resistance: A multicenter meta-analysis of the spectrum and frequencies, clinical behaviour, and phenotypic associations of resistance mechanisms. *Eur J Cancer*. 2015;51(18):2792-2799. doi: 10.1016/j.ejca.2015.08.022
20. Wang J, Sinnberg T, Niessner H, Dölker R, Sauer B, Kempf WE, Meier F, Leslie N, Schittek B. PTEN regulates IGF-1R-mediated therapy resistance in melanoma. *Pigment Cell Melanoma Res*. 2015;28(5):572-589. doi: 10.1111/pcmr.12390
21. Risson E, Nobre AR, Maguer-Satta V, Aguirre-Ghiso JA. The current paradigm and challenges ahead for the dormancy of disseminated tumor cells. *Nat Cancer*. 2020;1(7):672-680. doi: 10.1038/s43018-020-0088-5
22. Bollag G, Hirth P, Tsai J, Zhang J, Ibrahim PN, Cho H, Spevak W, Zhang C, Zhang Y, Habets G, Burton EA, Wong B, Tsang G, West BL, Powell B, Shellooe R, Marimuthu A, Nguyen H, Zhang KY, Artis DR, Schlessinger J, Su F, Higgins B, Iyer R, D'Andrea K, Koehler A, Stumm M, Lin PS, Lee RJ, Grippo J, Puzanov I, Kim KB, Ribas A, McArthur GA, Sosman JA, Chapman PB, Flaherty KT, Xu X, Nathanson KL, Nolop K. Clinical efficacy of a RAF inhibitor needs broad target blockade in BRAF-mutant melanoma. *Nature*. 2010 0;467(7315):596-599. doi: 10.1038/nature09454
23. Laphanuwat P., Likasitwatanakul P., Sittithumcharee G., Thaphaengphan A., Chomanee N., Suppramote O., Ketaroonrut N., Charngkaew K., Lam E.W., Okada S., Panich U., Sampattavanich S., Jirawatnotai S. Cyclin D1 depletion interferes with oxidative balance and promotes cancer cell senescence**.** *J Cell Sci*. 2018;131(12):jcs214726. doi: 10.1242/jcs.214726
24. Esimbekova AR, Palkina NV, Zinchenko IS, Belenyuk VD, Savchenko AA, Sergeeva EY, Ruksha TG. Focal adhesion alterations in G_0-positive melanoma cells. *Cancer Med*. 2023;12(6):7294-7308. doi: 10.1002/cam4.5510
25. Uxa S, Bernhart SH, Mages CFS, Fischer M, Kohler R., Hoffmann S., Stadler P.F., Engeland K., Müller G.A. DREAM and RB cooperate to induce gene repression and cell-cycle arrest in response to p53 activation. *Nucleic Acids Res*. 2019 6;47(17):9087-9103. doi: 10.1093/nar/gkz635
26. Indovina P., Marcelli E., Casini N., Rizzo V., Giordano A. Emerging roles of RB family: new defense mechanisms against tumor progression. *J Cell Physiol*. 2013;228(3):525-35. doi: 10.1002/jcp.24170
27. Milanovic M, Fan DNY, Belenki D, Däbritz JHM, Zhao Z, Yu Y, Dörr JR, Dimitrova L., Lenze D., Monteiro Barbosa IA, Mendoza-Parra MA, Kanashova T, Metzner M, Pardon K, Reimann M, Trumpp A, Dörken B, Zuber J, Gronemeyer H, Hummel M, Dittmar G, Lee S, Schmitt CA. Senescence-associated reprogramming promotes cancer stemness. *Nature*. 2018;553(7686):96-100. doi: 10.1038/nature25167

28. Fluegen G, Avivar-Valderas A, Wang Y, Padgen MR, Williams JK, Nobre AR, Calvo V, Cheung JF, Bravo-Cordero JJ, Entenberg D, Castracane J, Verkhusha V, Keely PJ, Condeelis J, Aguirre-Ghiso JA. Phenotypic heterogeneity of disseminated tumour cells is preset by primary tumour hypoxic microenvironments. *Nat Cell Biol*. 2017;19(2):120-132. doi: 10.1038/ncb3465

29. Aguirre-Ghiso JA, Liu D, Mignatti A, Kovalski K, Ossowski L. Urokinase receptor and fibronectin regulate the ERK(MAPK) to p38(MAPK) activity ratios that determine carcinoma cell proliferation or dormancy in vivo. *Mol Biol Cell*. 2001;12(4):863-79. doi: 10.1091/mbc.12.4.863

30. Zhang C, Wu M, Zhang L, Shang LR, Fang JH, Zhuang SM. Fibrotic microenvironment promotes the metastatic seeding of tumor cells via activating the fibronectin 1/secreted phosphoprotein 1-integrin signaling. *Oncotarget*. 2016;7(29):45702-45714. doi: 10.18632/oncotarget.10157

31. Ou J, Peng Y, Deng J, Miao H, Zhou J, Zha L, Zhou R, Yu L, Shi H, Liang H. Endothelial cell-derived fibronectin extra domain A promotes colorectal cancer metastasis via inducing epithelial-mesenchymal transition. *Carcinogenesis*. 2014;35(7):1661-1670. doi: 10.1093/carcin/bgu090

32. Han S, Khuri FR, Roman J. Fibronectin stimulates non-small cell lung carcinoma cell growth through activation of Akt/mammalian target of rapamycin/S6 kinase and inactivation of LKB1/AMP-activated protein kinase signal pathways. *Cancer Res*. 2006;66(1):315-323. doi: 10.1158/0008-5472.CAN-05-2367

33. Barbazán J, Alonso-Alconada L, Elkhatib N, Geraldo S, Gurchenkov V, Glentis A, van Niel G, Palmulli R, Fernández B, Viaño P, Garcia-Caballero T, López-López R, Abal M, Vignjevic DM. Liver metastasis is facilitated by the adherence of circulating tumor cells to vascular fibronectin deposits. *Cancer Res*. 2017;77(13):3431-3441. doi: 10.1158/0008-5472.CAN-16-1917

34. Li CL, Yang D, Cao X, Wang F, Hong DY, Wang J, Shen XC, Chen Y. Fibronectin induces epithelial-mesenchymal transition in human breast cancer MCF-7 cells via activation of calpain. *Oncol Lett*. 2017;13(5):3889-3895. doi: 10.3892/ol.2017.5896

35. Barbazan J, Pérez-González C, Gómez-González M, Dedenon M, Richon S, Latorre E, Serra M, Mariani P, Descroix S, Sens P, Trepat X, Vignjevic DM. Cancer-associated fibroblasts actively compress cancer cells and modulate mechanotransduction. *Nat Commun*. 2023;14(1):6966. doi: 10.1038/s41467-023-42382-4

36. Wang J, Zhang B, Wu H, Cai J, Sui X, Wang Y, Li H, Qiu Y, Wang T, Chen Z, Zhu Q, Xia H, Song W, Xiang AP. CD51 correlates with the TGF-beta pathway and is a functional marker for colorectal cancer stem cells. *Oncogene*. 2017; 36**:** 1351-1363. doi: 10.1038/onc.2016.299

37. Reimann M, Lee S, Schmitt CA. Cellular senescence: neither irreversible nor reversible. *J Exp Med*. 2024;221(4):e20232136. doi: 10.1084/jem.20232136